J|A|C|S COMMUNICATIONS

Published on Web 12/14/2010

Single-Molecule Junctions Based on Nitrile-Terminated Biphenyls: A Promising New Anchoring Group

Artem Mishchenko,[†] Linda A. Zotti,[‡] David Vonlanthen,[§] Marius Bürkle,[||] Fabian Pauly,[||] Juan Carlos Cuevas,*[,‡] Marcel Mayor,*[,§,⊥] and Thomas Wandlowski*[,†]

Department of Chemistry and Biochemistry, University of Bern, CH-3012 Bern, Switzerland, Departamento de Física Teórica de la Materia Condensada, Universidad Autónoma de Madrid, E-28049 Madrid, Spain, Department of Chemistry, University of Basel, CH-4056 Basel, Switzerland, Institut für Theoretische Festkörperphysik, Karlsruhe Institute of Technology, D-76131 Karlsruhe, Germany, and Institute for Nanotechnology, Karlsruhe Institute of Technology, D-76021 Karlsruhe, Germany

Received August 24, 2010; E-mail: juancarlos.cuevas@uam.es; marcel.mayor@unibas.ch; thomas.wandlowski@dcb.unibe.ch

Abstract: We present a combined experimental and theoretical study of the electronic transport through single-molecule junctions based on nitrile-terminated biphenyl derivatives. Using a scanning tunneling microscope-based break-junction technique, we show that the nitrile-terminated compounds give rise to well-defined peaks in the conductance histograms resulting from the high selectivity of the N−Au binding. Ab initio calculations have revealed that the transport takes place through the tail of the LUMO. Furthermore, we have found both theoretically and experimentally that the conductance of the molecular junctions is roughly proportional to the square of the cosine of the torsion angle between the two benzene rings of the biphenyl core, which demonstrates the robustness of this structure−conductance relationship.

The detailed understanding of charge transport through single-molecule junctions is a key prerequisite for the design and development of molecular electronic devices.[1,2] The implementation of (single) molecules in electronic circuits requires an optimization of their structures toward desired functionalities and a reliable method of wiring them into a nanoscale junction.[3−5] While it is generally recognized that organic molecules with π-conjugated cores are good candidates for molecular electronics applications,[4,6,7] the choice of a proper anchoring group constitutes a major challenge.[8−10] The terminal groups determine the strength of the binding to the adjacent leads as well as the energy and nature of the frontier molecular orbitals.[11] For example, electron-withdrawing groups attached to a π-conjugated system decrease the energies of both frontier orbitals and thereby promote electron transport by reducing the difference between the electrode's Fermi level and the molecule's LUMO. On the other hand, electron-donating substituents lift the frontier orbital energies and thus favor hole transport by bringing the molecule's HOMO closer to the Fermi level.[12,13] Furthermore, the spatial arrangement of a π-conjugated system is also crucial for the electronic transparence of a molecular junction.[14]

Thiol (−SH) groups are the anchoring groups most often used to connect (single) molecules to metal leads, such as gold electrodes, because of their high covalent bond strength.[15] However, the −SH terminus shows a large variability in its binding geometries.[9,16,17] Venkataraman et al.[18] recently introduced the amine group ($-NH_2$) as a promising alternative, one that is particularly characterized by a more uniform contact geometry.[19] Other anchoring groups that have been explored in (single) molecule conductance studies are pyridine,[20,21] isonitrile (−N≡C),[18,22] isothiocyanate (−N═C═S),[23] methyl selenide ($-SeCH_3$),[24] methyl thiol ($-SCH_3$),[24] dithiocarboxylic acid [−C(═S)−SH],[25] dimethylphosphine [$-P(CH_3)_2$],[24] carboxylic acid (−COOH),[15] nitro ($-NO_2$),[26] and even fullerene.[27] The search for the "best" anchoring group for the formation of stable and energetically well-aligned metal−molecule contacts represents one of the most important current issues in molecular electronics.[10,26,28]

In this communication, we report on a scanning tunneling microscope (STM) break-junction[17,20] study of electron transport in single-molecule junctions formed by a series of novel biphenyl dinitriles (BPDNs) (Table 1). An additional interlinking alkyl chain of varying length between the two phenyl subunits defines the torsion angle φ within this series of BPDNs, providing a molecular structural feature that is expected to be reflected in their transport properties.[29−31] These BPDN model compounds were obtained from precursors comprising terminal leaving groups,[32] and their synthesis will be reported elsewhere.[33] These chemically tailored molecules contact the gold leads through the electron-withdrawing nitrile (−C≡N) group. We note that −C≡N represents a unique and novel anchoring group that to the best of our knowledge has been explored in only two recent studies. Kiguchi et al.[34] attempted to measure the conductance of 1,4-dicyanobenzene but did not observe any clear molecular conductance signatures. Zotti et al.[26] performed measurements of the current−voltage characteristics of 4,4′-dicyanotolane molecules using a mechanically controllable break-junction technique, but no conductance histograms were reported.

In the present study, we created contacts between a gold STM tip and a Au(111) substrate and then measured the conductance $G = I/V_{bias}$ in the tip−substrate junction as a function of the relative tip−substrate separation z upon stretching and breaking of these contacts in the presence of BPDN target molecules. The experimental data were analyzed with novel statistical approaches based on 2D histograms and a covariance matrix representation. Details of the experimental technique and data analysis procedures are summarized in the Supporting Information (SI).

As an example, Figure 1a shows typical conductance−distance curves obtained in the presence of molecule M4. The plateaus of rather constant conductance observed in these stretching traces around $1 \leq G/G_0 \leq 10$, where $G_0 = 2e^2/h$, correspond to stable atomic contacts, while the ones in the range $10^{-5} \leq G/G_0 \leq 10^{-4}$ represent the signatures of molecular junctions. We did not observe signatures corresponding to binding of multiple molecules in the

[†] University of Bern.
[‡] Universidad Autónoma de Madrid.
[§] University of Basel.
[||] Institut für Theoretische Festkörperphysik, Karlsruhe Institute of Technology.
[⊥] Institute for Nanotechnology, Karlsruhe Institute of Technology.

 10.1021/ja107340t

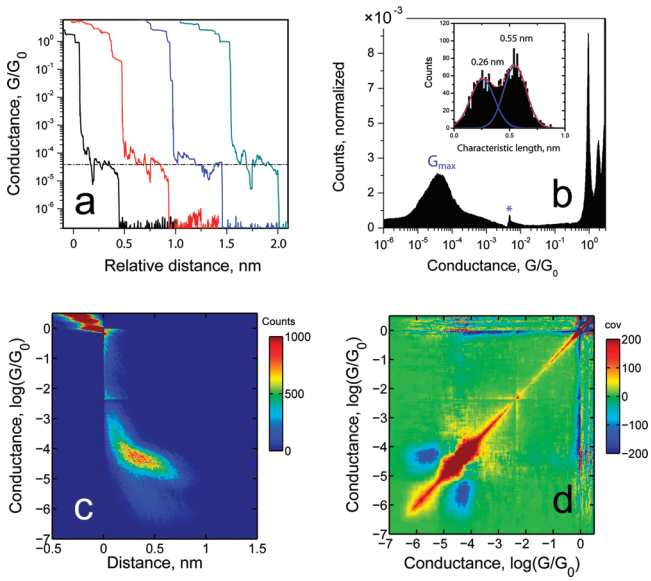

Figure 1. (a) Selected experimental stretching curves (shifted horizontally for clarity). (b) 1D logarithmic conductance histogram and (inset) characteristic length histogram; (c) 2D conductance−distance histogram. (d) Covariance matrix. All traces shown were measured using a 1 mM solution of M4 in 4:1 (v/v) mesitylene/THF at $V_{bias} = 100$ mV and processed without any data selection.

junction and thus conclude that most of the traces with molecular features contain only a single plateau. The main panel in Figure 1b displays the corresponding one-dimensional (1D) histogram on a logarithmic conductance scale constructed from ∼2000 individual stretching traces of M4. The sharp peaks in the histogram around integer multiples of G_0 represent the conductance of gold quantum point contacts.[35] The prominent peak with a maximum at $G_{max}/G_0 = 4 \times 10^{-5}$ is attributed to the most probable conductance of a single M4 molecule bound to two gold electrodes. (The feature near $G/G_0 = 5 \times 10^{-3}$ results from a known instrumental artifact. For details, see the SI.)

The inset in Figure 1b shows the characteristic length histogram of M4, which was constructed by measuring the lengths of all of the individual conductance−distance traces in the molecular junction conductance range around G_{max}, typically within the interval $0.1 \le G/G_{max} \le 10$. We found two distinct peaks at 0.26 and 0.55 nm. The first, which is dependent on the lower limit of the interval for data analysis, represents the average tip movement between $G/G_{max} = 0.1$ and 10 in the absence of a molecular junction. The second value is asserted to be the "true" average length of a molecular plateau or, in other words, the relative distance between the formation and breaking of a single-molecule junction (for details, see the SI).

The above interpretation is further supported by a two-dimensional (2D) histogram[27] representation. Figure 1c shows the logarithm of the experimentally obtained conductance of M4 in units of G_0 plotted versus distance. It should be noted that we introduced a relative distance scale z' (with $z' = 0$ at $G = 0.7G_0$) to normalize the experimental traces to a common point. The chosen procedure was justified because of the steep decay of the tunneling current after breaking of the last atomic contact. The histogram was obtained by counting the occurrence of $[\log(G/G_0), z']$ pairs in a 2D field. Figure 1c shows features of gold quantum contacts at $G \ge G_0$ and a second cloud-like pattern in the $[10^{-5} \le G/G_0 \le 10^{-4}, 0 \le z' \le 0.5$ nm] region. We attribute the latter to the formation of single-molecule junctions of only one type. The center of the cloud is located at $G = (3.5-4.5) \times 10^{-5}G_0$, which is close to the position of the peak in the 1D histogram (Figure 1b). The extension of the cloud along the distance scale is ∼0.5 nm, close to the position of the second peak in the plateau length histogram (inset in Figure 1b). A small number of counts below the cloud were due to the steep curves without molecular plateaus.

Inspired by Halbritter et al.,[36] we for the first time applied a covariance analysis to features in a molecular conductance histogram (for details, see the SI). The covariance provides a measure of the strength of a correlation between pairs of bins in the histogram. The covariance is 0 if the variations of counts in two different bins are independent, positive if they are correlated, and negative if they are anticorrelated. The matrix of covariance values of M4 is plotted in Figure 1d. The strongly correlated bins (red color) along the diagonal of the matrix at $\log(G/G_0) \ge -1$ appear from the plateaus of the Au−Au atomic junctions. The positive values at $-5 \le \log(G/G_0) \le -3.5$ are attributed to the conductance plateaus of the single-molecule junctions. The strong anticorrelation (blue color) in the area $[\log(G/G_0) \approx 0, -4 \le \log(G/G_0) \le 0]$ followed by a smaller correlation feature at $[\log(G/G_0) \approx 0, -5 \le \log(G/G_0) \le -4]$ indicates that conductance plateaus of both atomic and molecular junctions are present in the majority of the original curves and that they are well-separated by the steep decrease in the conductance. The strong anticorrelation in the area $[-5 \le \log(G/G_0) \le -4, -6 \le \log(G/G_0) \le -5]$ is due to the steep decay of the current after the molecular junctions were broken.

Table 1. Chemical Structures of the Studied Molecules, Values of the Torsion Angle between the Two Phenyl Rings (φ) Obtained from X-ray Experiments with Single Crystals (M2−M6)[33] or DFT Calculations (M1), and Measured Values of the Most Probable Single-Molecule Conductances

Molecule	Structure	φ (deg)	Conductance (G_0)
M1	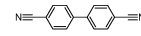	35.5	$(4.7 \pm 0.6) \cdot 10^{-5}$
M2	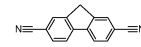	1.0	$(9.2 \pm 1.7) \cdot 10^{-5}$
M3	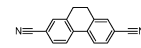	20.7	$(6.6 \pm 0.6) \cdot 10^{-5}$
M4	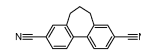	44.8	$(3.9 \pm 0.5) \cdot 10^{-5}$
M5	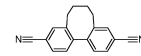	58.5	$(1.7 \pm 0.2) \cdot 10^{-5}$
M6	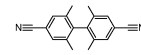	89.3	$< 10^{-6}$

We further explored the dependence of the single-molecule conductances on the torsion angle between the two phenyl rings, φ, by choosing a series of five additional BPDN derivatives (Table 1). The angles φ, as obtained from X-ray structure analysis of the molecular single crystals (M2−M6) or DFT calculations (M1), varied systematically between 1 and 89° while the molecular length remained approximately constant.[33] The individual experiments and the corresponding data analysis followed the protocol described for M4. We note that the entire statistical analysis of all of the measured traces was performed without any data selection. This is in strong contrast to experiments with thiol-bound molecules, where an appropriate data selection procedure is needed to extract meaningful results.[17,30,37,38]

Qualitatively similar results were obtained for all six BPDN derivatives. Each of the 1D conductance histograms exhibited only one dominant molecular-junction-related maximum. The 2D conductance−distance histograms and the covariance matrices also revealed only one molecular feature (see the SI). The experimentally

measured values of the corresponding most probable single-molecule conductances are summarized in Table 1 and plotted in Figure 2a as a function of $\cos^2 \varphi$. The conductances of the derivatives (except for fluorene M2, for which the value lies above the general trend) were approximately proportional to $\cos^2 \varphi$, with a slope of $(7.3 \pm 0.2) \times 10^{-5} G_0$. This slope is smaller than those reported for biphenyl derivatives with thiol $[(2.4 \pm 0.1) \times 10^{-4} G_0]$[30] or amine $(1.5 \times 10^{-3} G_0)$[29] anchoring groups.

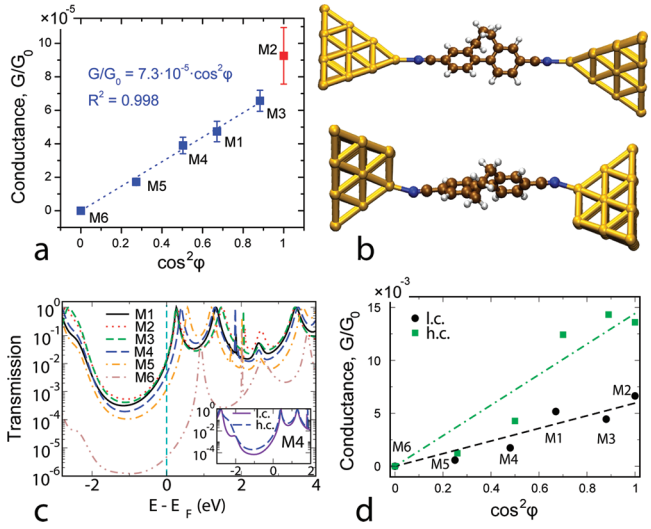

Figure 2. (a) Experimentally measured conductances G/G_0 of six biphenyl dinitriles as a function of the square of the cosine of the torsion angle, $\cos^2 \varphi$ (Table 1). For molecule M6, the conductance was set equal to zero. (b) Optimized geometries of molecule M4 connected at both ends to Au⟨111⟩ electrodes in the (upper panel) l.c. and (lower panel) h.c. geometries. (c) Transmission as a function of energy (with respect to the Fermi energy, E_F) for all of the molecules in the h.c. geometry. The inset shows a comparison of the transmission curves for M4 bound in the h.c. (solid curve) and l.c. (dashed curve) geometries. (d) Computed conductances of M1−M6 as functions of $\cos^2 \varphi$ for the two contact geometries.

To provide further insight into the experimental results, we carried out ab initio calculations on the structures and zero-bias conductances of the molecular junctions. For this purpose, we combined density functional theory (DFT) and the Landauer formalism[39] (see the SI for details). We first analyzed all of the "free" molecules in the gas phase and compared the energies of the frontier orbitals. We found a monotonic decrease of the HOMO−LUMO gap with decreasing torsion angle without a particular deviation for the fluorene derivative M2 (see Figure S23 in the SI). Thus, our calculations could not explain the deviation observed experimentally (Figure 2a). Subsequently, we studied the structure of the entire gold−molecule−gold junction, with the two leads represented by relaxed 20-atom-sized gold clusters that were subsequently extended to 120 atoms after geometry optimization. We explored various binding geometries (specifically atop, hollow, and bridge) and found that only atop binding geometries of the nitrile−gold contact are stable. This result is due to the coordinative nature of the covalent N−Au bond, which is established via the nitrogen lone pair. We focus here on two representative atop structures. In the first one (denoted as the l.c. geometry; Figure 2b, upper panel), the molecule is bound to a low-coordination-number gold adatom through a linear C−N−Au bond. In the second one (denoted as the h.c. geometry; Figure 2b, lower panel), the BPDN molecule attaches to a "terrace-type" gold atom with a higher coordination number, and the C−N−Au angle assumes a value of ∼160°. The binding energies for the two geometries are very similar (∼1 eV; see the SI).

Further, we calculated the transmission curves at zero bias for M1−M6 in the l.c. and h.c. geometries (Figure 2c). In all cases, we found that the transport takes place through the tail of the LUMO (off-resonant tunneling). This is consistent with the results of previous calculations[11,26] and thermopower measurements[40] in nitrile-terminated molecular junctions. The transmission curves for the h.c. geometry show an approximately 20 meV broader transmission resonance at a slightly lower energy (by ∼20 meV) than for the l.c. geometry (see the comparison for molecule M4 in the inset of Figure 2c) for all of the molecules. The energy difference between the first two transmission resonances above the Fermi energy was found to decrease with increasing torsion angle, which is in agreement with results reported for biphenyl dithiols in ref 30.

The computed values of the junction conductances are plotted in Figure 2d as a function of the square of the cosine of the calculated torsion angle. The dashed lines represent the linear fit $G = a \cos^2 \varphi$. The slope for the h.c. geometry ($a = 1.44 \times 10^{-2} G_0$) is higher than that obtained for the l.c. geometry ($a = 5.9 \times 10^{-3} G_0$) because a better coupling between the molecular π system and the metal states yields a broader resonance in the former case. The computed conductance values are 2 orders of magnitude higher than the experimental ones, which is mostly due to the underestimation of the HOMO−LUMO gap by DFT.[8,13] We note that both the experimental and theoretical conductances obtained for the BPDN family are lower than the values reported for biphenyl dithiols.[30] We find that this is due to a lower coupling (by a factor of ∼3) in the case of the BPDN derivatives relative to the biphenyl dithiols, and we attribute this to the presence of one more atom in nitrile than in thiol, which acts as a spacer.

In order to evaluate whether the room temperature can affect the molecular structures and in turn the conductance values, we performed molecular dynamics (MD) simulations for the isolated molecules at 300 K in both vacuum and a solvent environment (see the SI). They revealed that the torsion angles fluctuate around the equilibrium values. The magnitude of these fluctuations depends on steric effects and on the internal strain in the molecule. The highest variation was found for M1, and it amounts to ±13°. The corresponding variation of the conductance due to fluctuations of the torsion angle was then estimated to be up to 24% (see the SI). It is worth noticing that the variations in the computed conductances due to the two different binding geometries and the fluctuations in the torsion angles lie well within the experimental spread. This spread covers a range of ∼1 order of magnitude and contains additional contributions from junction stretching, which was not considered in the theoretical modeling. Thus, the coexistence of the two calculated binding geometries in the experimental data is highly probable. These findings support the experimental observation of a single conductance peak for the nitrile terminated molecules. Indeed, on the basis of our experimental data, we can state that the nitrile-bound junctions show a strong structural selectivity and are more uniform than, for example, thiol-based ones.[17,30,37]

To gain further insight into the nature of the transport through these molecules, we also analyzed the contributions of the individual conduction channels to the total conductance. We found that for the different molecules the conductance is dominated by a single channel, except in the case of M6, where two channels give almost the same contribution. Analysis of the wave functions of the dominant channels revealed that for M1−M5 they have π character and symmetries resembling those of the LUMOs of the isolated molecules, while for M6 the two channels have mixed $\pi-\sigma$

character because of the complete breaking of the conjugation of the π system.

To conclude, we have studied the conductance of a family of biphenyl derivatives wired to gold electrodes via nitrile anchoring groups. 1D and 2D conductance histograms as well as covariance matrix analysis exhibited well-defined features that we attribute to a site-selective N−Au bond. We experimentally and theoretically observed a decrease in the single-molecule conductance with increasing torsion angle φ. The high probability of spontaneously forming gold−nitrile bonds, as demonstrated by our results in this communication, constitutes another important advantage of the nitrile-terminated molecules. These findings indicate that nitrile-based metal−molecule−metal junctions represent a unique platform for the reliable construction of nanoscale molecular assemblies with very uniform electric properties.

Acknowledgment. The authors are grateful to I. V. Pobelov for helpful comments. L.A.Z. and J.C.C. were funded by the EU through the BIMORE Network (MRTN-CT-2006-035859). F.P. and M.B. acknowledge funding through a Young Investigator Group and the DFG, respectively. A.M. and T.W. acknowledge support from the Swiss National Science Foundation (200021_124643; NFP62), the ITN FP7 Network FUNMOLS, and DFG Priority Program 1243. D.V. and M.M. acknowledge support from the Swiss National Science Foundation, the Swiss Nanoscience Institute, and the National Center of Competence in Nanoscale Sciences.

Supporting Information Available: Experimental setup, procedure, analysis, experimental data, and details of the calculations. This material is available free of charge via the Internet at http://pubs.acs.org.

References

(1) Nitzan, A.; Ratner, M. A. *Science* **2003**, *300*, 1384–1389.
(2) Joachim, C.; Gimzewski, J. K.; Aviram, A. *Nature* **2000**, *408*, 541–548.
(3) Chen, F.; Hihath, J.; Huang, Z.; Li, X.; Tao, N. *Annu. Rev. Phys. Chem.* **2007**, *58*, 535–564.
(4) Moth-Poulsen, K.; Bjørnholm, T. *Nat. Nanotechnol.* **2009**, *4*, 551–556.
(5) van der Molen, S. J.; Liljeroth, P. *J. Phys.: Condens. Matter* **2010**, *22*, 133001.
(6) Salomon, A.; Cahen, D.; Lindsay, S.; Tomfohr, J.; Engelkes, V.; Frisbie, C. *Adv. Mater.* **2003**, *15*, 1881–1890.
(7) Huber, R.; Gónzalez, M. T.; Wu, S.; Langer, M.; Grunder, S.; Horhoiu, V.; Mayor, M.; Bryce, M. R.; Wang, C.; Jitchati, R.; Schönenberger, C.; Calame, M. *J. Am. Chem. Soc.* **2008**, *130*, 1080–1084.
(8) Lindsay, S.; Ratner, M. *Adv. Mater.* **2007**, *19*, 23–31.
(9) Kristensen, I. S.; Mowbray, D. J.; Thygesen, K. S.; Jacobsen, K. W. *J. Phys.: Condens. Matter* **2008**, *20*, 374101.
(10) Dell'Angela, M.; Kladnik, G.; Cossaro, A.; Verdini, A.; Kamenetska, M.; Tamblyn, I.; Quek, S. Y.; Neaton, J. B.; Cvetko, D.; Morgante, A.; Venkataraman, L. *Nano Lett.* **2010**, *10*, 2470–2474.
(11) Xue, Y.; Ratner, M. A. *Phys. Rev. B* **2004**, *69*, 085403.
(12) Venkataraman, L.; Park, Y. S.; Whalley, A. C.; Nuckolls, C.; Hybertsen, M. S.; Steigerwald, M. L. *Nano Lett.* **2007**, *7*, 502–506.
(13) Cuevas, J. C.; Scheer, E. *Molecular Electronics: An Introduction to Theory and Experiment*; World Scientific: Singapore, 2010.
(14) Woitellier, S.; Launay, J.; Joachim, C. *Chem. Phys.* **1989**, *131*, 481–488.
(15) Chen, F.; Li, X.; Hihath, J.; Huang, Z.; Tao, N. *J. Am. Chem. Soc.* **2006**, *128*, 15874.
(16) Müller, K.-H. *Phys. Rev. B* **2006**, *73*, 045403.
(17) Li, C.; Pobelov, I.; Wandlowski, T.; Bagrets, A.; Arnold, A.; Evers, F. *J. Am. Chem. Soc.* **2008**, *130*, 318–326.
(18) Venkataraman, L.; Klare, J. E.; Tam, I. W.; Nuckolls, C.; Hybertsen, M. S.; Steigerwald, M. L. *Nano Lett.* **2006**, *6*, 458.
(19) Hybertsen, M. S.; Venkataraman, L.; Klare, J. E.; Whalley, A. C.; Steigerwald, M. L.; Nuckolls, C. *J. Phys.: Condens. Matter* **2008**, *20*, 374115.
(20) Xu, B.; Tao, N. J. *Science* **2003**, *301*, 1221–1223.
(21) Kamenetska, M.; Quek, S. Y.; Whalley, A. C.; Steigerwald, M. L.; Choi, H. J.; Louie, S. G.; Nuckolls, C.; Hybertsen, M. S.; Neaton, J. B.; Venkataraman, L. *J. Am. Chem. Soc.* **2010**, *132*, 6817–6821.
(22) Kim, B.; Beebe, J. M.; Jun, Y.; Zhu, X.-Y.; Frisbie, C. D. *J. Am. Chem. Soc.* **2006**, *128*, 4970–4971.
(23) Ko, C.-H.; Huang, M.-J.; Fu, M.-D.; Chen, C.-H. *J. Am. Chem. Soc.* **2010**, *132*, 756–764.
(24) Park, Y. S.; Whalley, A. C.; Kamenetska, M.; Steigerwald, M. L.; Hybertsen, M. S.; Nuckolls, C.; Venkataraman, L. *J. Am. Chem. Soc.* **2007**, *129*, 15768–15769.
(25) Xing, Y.; Park, T.-H.; Venkatramani, R.; Keinan, S.; Beratan, D. N.; Therien, M. J.; Borguet, E. *J. Am. Chem. Soc.* **2010**, *132*, 7946–7956.
(26) Zotti, L. A.; Kirchner, T.; Cuevas, J. C.; Pauly, F.; Huhn, T.; Scheer, E.; Erbe, A. *Small* **2010**, *6*, 1529–1535.
(27) Martin, C. A.; Ding, D.; Sørensen, J. K.; Bjørnholm, T.; van Ruitenbeek, J. M.; van der Zant, H. S. J. *J. Am. Chem. Soc.* **2008**, *130*, 13198.
(28) Kiguchi, M.; Tal, O.; Wohlthat, S.; Pauly, F.; Krieger, M.; Djukic, D.; Cuevas, J. C.; van Ruitenbeek, J. M. *Phys. Rev. Lett.* **2008**, *101*, 046801.
(29) Venkataraman, L.; Klare, J. E.; Nuckolls, C.; Hybertsen, M. S.; Steigerwald, M. L. *Nature* **2006**, *442*, 904–907.
(30) Mishchenko, A.; Vonlanthen, D.; Meded, V.; Bürkle, M.; Li, C.; Pobelov, I. V.; Bagrets, A.; Viljas, J. K.; Pauly, F.; Evers, F.; Mayor, M.; Wandlowski, T. *Nano Lett.* **2010**, *10*, 156–163.
(31) Vonlanthen, D.; Mishchenko, A.; Elbing, M.; Neuburger, M.; Wandlowski, T.; Mayor, M. *Angew. Chem., Int. Ed.* **2009**, *48*, 8886–8890.
(32) Vonlanthen, D.; Rotzler, J.; Neuburger, M.; Mayor, M. *Eur. J. Org. Chem.* **2010**, 120–133.
(33) Vonlanthen, D.; Rudnev, A.; Mishchenko, A.; Käslin, A.; Rotzler, J.; Neuburger, M.; Wandlowski, T.; Mayor, M. *Phys. Chem. Chem. Phys.*, submitted for publication.
(34) Kiguchi, M.; Miura, S.; Hara, K.; Sawamura, M.; Murakoshi, K. *Appl. Phys. Lett.* **2006**, *89*, 213104.
(35) Agraït, N.; Yeyati, A. L.; van Ruitenbeek, J. M. *Phys. Rep.* **2003**, *377*, 81–279.
(36) Halbritter, A.; Makk, P.; Mackowiak, S.; Csonka, S.; Wawrzyniak, M.; Martinek, J. Atom by Atom Narrowing of Transition Metal Nanowires Resolved by 2D Correlation Analysis. 2010, arXiv/1006.1811. arXiv.org e-Print archive. http://arxiv.org/abs/1006.1811 (accessed Aug 24, 2010).
(37) Li, X.; He, J.; Hihath, J.; Xu, B.; Lindsay, S. M.; Tao, N. *J. Am. Chem. Soc.* **2006**, *128*, 2135–2141.
(38) Haiss, W.; Nichols, R. J.; van Zalinge, H.; Higgins, S. J.; Bethell, D.; Schiffrin, D. J. *Phys. Chem. Chem. Phys.* **2004**, *6*, 4330–4337.
(39) Pauly, F.; Viljas, J. K.; Huniar, U.; Häfner, M.; Wohlthat, S.; Bürkle, M.; Cuevas, J. C.; Schön, G. *New J. Phys.* **2008**, *10*, 125019.
(40) Baheti, K.; Malen, J. A.; Doak, P.; Reddy, P.; Jang, S.-Y.; Tilley, T. D.; Majumdar, A.; Segalman, R. A. *Nano Lett.* **2008**, *8*, 715–719.

JA107340T